KERNFORSCHUNGSZENTRUM

KARLSRUHE

September 1967

KFK 667
EUR 3700 e

Institut für Angewandte Reaktorphysik

Automatic Control System for Balanced Oscillator Tests

M. Audoux, L. Caldarola, P. Giordano, H. Rohrbacher

GESELLSCHAFT FUR KERNFORSCHUNG M.B.H.

KARLSRUHE

KERNFORSCHUNGSZENTRUM KARLSRUHE

September 1967

K F K 667
EUR 3700 e

Institut für Angewandte Reaktorphysik

Automatic Control System for Balanced Oscillator Tests*

by

M. Audoux** ***
L. Caldarola**
P. Giordano** ***
H. Rohrbacher***

Gesellschaft für Kernforschung m.b.H., Karlsruhe

* Work performed within the association in the field of fast reactors between the European Atomic Energy Community and Gesellschaft für Kernforschung m.b.H.,Karlsruhe.

** EURATOM, Brussels, delegated to the Karlsruhe Fast Breeder Project, Kernforschungszentrum Karlsruhe.

*** Institut für Reaktorentwicklung, Kernforschungszentrum Karlsruhe.

Abstract

It has been demonstrated that the Balanced Oscillator Tests are more convenient than the traditional oscillator tests, because they allow to get more complete and precise informations on reactor parameters such as reactivity coefficients, fuel time constant etc.. A special automatic control system to carry out these experiments has been developed, built and tested on the analog computer.

It has been planned to use this type of automatic control system to perform Balanced Oscillator Tests on SEFOR (Southwest Experimental Fast Oxide Reactor).

Contents

1. Introduction

2. Generals

3. Basic design criteria

4. Results of the studies on the analog computer

5. Practical realization of the system

6. Final Considerations

7. References

8. Appendix 1: "Approximate Evaluation of the behaviour of the controlled variable in the time domain

9. Appendix 2: Dependence of the precision upon the error "$\delta\psi$" of phase setting

1. Introduction

It has been demonstrated that the "Balanced Oscillator Tests" are more convenient than the traditional oscillator tests, because they allow to get more complete and precise informations on reactor parameters such as reactivity coefficients, fuel time constant etc..

Fig. 1-1A shows a schematic block diagram of a plant (for example a nuclear plant). If we oscillate an input variable alone (for example the reactivity), there will be many variables (power and coolant temperatures) which will oscillate. Each one of these variables will produce reactivity feedbacks with associated time constants. The transfer function between power and reactivity will contain all these effects, so that the results, obtainable from the analysis of these measurements, will not be very precise.

Fig. 1-1B shows a schematic diagram of the 1st Balanced Oscillator Test (B.O.T.). The two controllers provide to keep the coolant temperatures constant by oscillating primary and secondary coolant flows. The transfer function between power and reactivity is now a cleaner function, because it contains only two parameters to be determined: the reactivity power coefficient and the fuel time constant. The transfer function between power and primary coolant flow can also

be measured and this gives additional informations on fuel thermal parameters (Ref. 1). A second B.O.T. is also possible (Fig. 1-1C), in which the power is kept constant and the transfer function between reactivity and average coolant temperature is measured. This gives the possibility to evaluate the fuel and coolant reactivity coefficients (Ref. 2).

The "Balanced Oscillator Tests" may be useful also for the measurement of transfer functions of any type of plant for control purposes. For these reasons, it was decided at Karlsruhe to develop a special type of automatic control system to carry out these tests in the most precise and fast way (Ref. 6). A prototype of this automatic control system has been already built and tested on the analog computer.

Balanced Oscillator Tests are planned for SEFOR (Southwest Experimental Fast Oxide Reactor) where an automatic control system of the type described in this paper will be used (Ref. 6).

2. Generals

Fig. 2-1A shows a schematic block diagram of the connections of the Automatic Control System to the SEFOR plant in the case of the 1st Balanced Oscillator Test (B.O.T.).

The heat produced in the core is removed by the primary coolant, Sodium, and is then transferred to the secondary Sodium circuit. From here the heat is rejected to the atmosphere by open circuit forced air cooling.

The reactor is fed with a sinusoidal reactivity signal at frequency "f_o"

$$\Delta K = \Delta K_m \sin 2\pi f_o t \qquad (1)$$

which is produced by the "Frequency and Sinus Function Generator". The input signal to the "Controller Nr. 1" is the difference between the signal of outlet and inlet reactor coolant temperatures, $(\Theta_{out} - \Theta_i)$. Its output signal acts on the "Primary Pump", which will tend to change the primary Sodium flow in such a way that

$$\Theta_{out} - \Theta_i = \text{const.} \qquad (2)$$

The input signal to the "Controller No. 2" is the outlet primary heat exchanger Sodium temperature, T_{out}. Its output signal acts on the "Secondary Pump" which

will tend to change the secondary coolant flow in such a way that

$$T_{out} = \text{const.} \tag{3}$$

The Transfer Function Analyser (T.F.A.) measures the transfer functions respectively between power (P) and reactivity (Δk) and between primary coolant flow (Δw_p) and power (P).

An alternative to the scheme of Fig. 2-1A is that of Fig. 2-1B in which the input to "Controller No. 1" is the signal of the outlet reactor coolant temperature "Θ_{out}".

Fig. 2-2A shows a schematic block diagram of the connections of the Closed Loop Control System to the plant in the case of the 2nd B.O.T.

The plant is fed with a sinusoidal signal at frequency "f_o" on the primary pump

$$\Delta w_p = \Delta w_{pm} \sin (2 \pi f_o t) \tag{4}$$

The secondary pump can either be controlled to keep "T_{out}" constant (as in the 1st B.O.T.) or be fed with a sinusoidal signal.

$$\Delta w_s = \Delta w_{sm} \sin(2 \pi f_o t + \alpha) \tag{5}$$

with Δw_{pm} and "α" chosen in such a way that they produce the maximum possible change of the reactor average coolant temperature, $\Delta\bar{\Theta}$, compatibly with the safety and the limitations of the plant. Both the possible control schemes of the secondary pump have not been shown in Fig. 2-2A.

The input signal to the "Controller" is the power, P, which is measured by a flux detector. Its output signal acts on a control rod to produce a change of reactivity, Δk, which will tend to keep the power constant

$$P = \text{const.} \tag{6}$$

The T.F.A. measures the transfer function between the reactivity (Δk) and the average coolant temperature ($\bar{\Theta}$) so defined:

$$\bar{\Theta} = \frac{\Theta_i + \Theta_{out}}{2} \tag{7}$$

An alternative to the scheme of Fig. 2-2A is that of Fig. 2-2B in which the power P is kept constant by acting on the primary coolant flow.

3. Basic Design Criteria

Each of the control loops of figs. 2-1A, 2-1B, 2-2A and 2-2B can be schematically described by the diagram shown in fig. 3-1. In fig. 3-1 "U" is the controlled variable which is intended to be kept constant. When an input signal "I" is introduced in the plant, this will produce a change "U_1" of U through the transfer function $P_1(s)$. The controlled variable "U" is measured by the "Feedback" circuit which has the transfer function "H(s)". The output signal "Y" from this circuit is compared to the reference "R" and the difference "ε" feeds the "Controller". The output signal "γ" from the Controller acts on the plant and produces a change "U_2" of "U" which tends to compensate for the previous change "U_1" due to the input signal "I". The plant transfer function between U_2 and γ is indicated with $P_2(s)$.

The Controller consists of two parts which we call "Regulator" and High Gain Unit (H.G.U.) having respectively transfer functions G(s) and M(s).

The function of the "Regulator" is to amplify the input signal "ε".

The function of the "High Gain Unit" is to suppress the oscillations of the controlled variable "U" at the frequency "f_o" at which the B.O.T. is performed. This means that any disturbance "U_1" of U at the frequency "f_o" is compensated by an oscillation "U_2" having the same amplitude of U_1.

The H.G.U. can be connected or disconnected from the loop, by operating the switch "S_w" (fig. 3-1) without effecting the stability of the system.

Looking at fig. 3-1 we can write the following equations in the Laplace domain

$$U = U_1 + U_2 \tag{1}$$

$$U_2 = \gamma P_2(s) \tag{2}$$

$$\gamma = \eta + \lambda \tag{3}$$

$$\lambda = \gamma M(s) \tag{4}$$

$$\eta = \varepsilon G(s) \tag{5}$$

$$\varepsilon = R - Y \tag{6}$$

$$Y = U H(s) \tag{7}$$

From eqs. 2 to 7 we get (for R = const):

$$\frac{U_2}{U} = - K(s) \tag{8}$$

where

$$K(s) = w(s) \frac{1}{1-M(s)} \tag{9}$$

and

$$w(s) = P_2(s) \cdot H(s) \cdot G(s) \tag{10}$$

From eqs. 1 and 8, we get

$$\frac{U}{U_1} = \frac{1}{1+K(s)} \tag{11}$$

The transfer function of eq. 11 is called "closed loop transfer function", while that of eq. 8 is called "open loop transfer function". The reason of the second denomination is due to the fact that eq. 8 would represent the transfer function of the loop supposed to be ideally cut at the point where U_1 and U_2 are added.

From eqs. 8 and 11 it is clear that the properties of the closed loop transfer function "$\frac{U}{U_1}$" can be derived by analysing the open loop transfer function "K(s)".

Curve No. 1 of Fig. 3-2 shows the polar diagram of the frequency response of the function

$$W(j2\pi f) = P_2(j2\pi f)\ H(j2\pi f)\ G(j2\pi f) \tag{12}$$

in a particular numerical case.

Let us suppose for a moment that the H.G.U. (fig. 3-1) is a "Low Pass Filter" (L.P.F.). If the input signal "γ" is at low frequency, it will pass through the filter and the output "λ" will be added to the signal "η" from the "Regulator". If instead "γ" is at higher frequency, it will be attenuated and shifted by the filter and therefore the output signal "λ" will not have practically any regulating action.

This means that the controller would be able to give a precise control at low frequencies, while at higher frequencies instead would become less accurate.

This loss of accuracy is due to two causes

a) the higher is the frequency, the more delayed in phase is the signal "λ" in respect to "η"

b) the higher is the frequency, the bigger is the attenuation between "λ" and "γ".

The first cause can be eliminated by making a phase correction with a device which changes the phase without changing the amplitude, for example a pure time delay.

If we incorporate in our H.G.U. a memory in cascade to the "Low Pass Filter", the frequency response of the transfer function M(s) would be of the type:

$$M(j2\ f) = A\ \frac{\exp(-j\ \psi f/f_o)}{(1+j\ f/f_m)^n} \qquad (13)$$

where "f_m" is the out-off frequency of the filter.

The angle "ψ" must be chosen in such a way that, at the frequency "f_o" of the experiment, the sum of "ψ" and of the phase shift "ϕ_o" due to the filter gives 2π, that is

$$\psi + \phi_o = 2\pi \qquad (14)$$

The curve of Fig. 3-3 shows the polar diagram of the frequency response of

$$\frac{1}{1-M(j\ f/f_o)} \qquad (15)$$

as function of "$\frac{f}{f_o}$" where M(s) is given by eq. 13 with

$$n=4\ , \qquad \frac{f_o}{f_m} = 0.2 \quad \text{and } A = 1 \qquad (16)$$

This curve shows an high gain at the frequency "f_o". At the higher harmonics $2f_o$, $3f_o$ etc., the gain presents also a maximum value which is becoming smaller as the order of the harmonic increases.

If we now introduce this modified H.G.U. in our control loop, the frequency response of the open loop transfer function K(j2πf) becomes the curve No. 2 of Fig. 3-2 if the system is set at the frequency

$$f_o = 0.02 \text{ cps.} \qquad (17)$$

The gain at frequency "f_o" is about 12.5, which means that the oscillation amplitude of the controlled variable "U" at this frequency is reduced to $\frac{1}{12.5} = 8\%$ of that of the disturbance "U_1". The curve No. 2 of fig. 3-2 shows (according to the Nyquist criterion) that the closed loop will be stable because the open loop

transfer function does not encircle the point "-1". This conclusion can be easily drawn if one thinks that stability means that the characteristic transcendental equation of the closed loop

$$w(s)\frac{1}{1-M(s)}+1=0 \qquad (18)$$

must not have any root with real part positive. If one puts in eq. 20

$$s = \alpha + j\ 2\pi\ f \qquad (19)$$

for $\alpha > 0$ one realizes that, for the same value of "f", the function w(s) becomes smaller in modulus and phase shift. This means that, for a given frequency, the corresponding point on the curve (curve No. 1 of fig. 3-2) tends to move from the left to the right (as indicated by the small arrow), while the curve tend to squeeze itself towards the origin. At the same time the function $1/\lfloor 1-M(s) \rfloor$ of fig. 3-3 tends, for $\alpha > 0$, to squeeze itself towards the point "1". Because of all these effects, the envelope of the lobes of curve No. 2 in fig. 3-2, for $\alpha > 0$, tends to squeeze itself towards the origin. This behaviour of the function $w(s)/\lfloor 1-M(s) \rfloor$ seen on the Nyquist diagram (curve No. 2 of fig. 3-2) ensures us that the characteristic equation 20 is always (for $\alpha \geq 0$) different from -1

$$w(s)\ \frac{1}{1-M(s)} \neq -1 \qquad (20)$$

This means that the system is stable. In order to improve the accuracy of the system, one can use a L.P.F. with a damping factor "ζ" different from 1. The frequency response of the transfer function "M(s)" of the H.G.U. would be of the type

$$M(j2\ f) = A\ \frac{\exp(-j\ \psi\ f/f_o)}{\left[1+2j\ \zeta\ f/f_m-(f/f_m)^2\right]^n} \qquad (21)$$

The damping faktor "ζ" must be chosen in such a way that the modulus of $M(j2\pi f)$ has its maximum value at $f = f_o$. "A" is then chosen so that the modulus "C" of $M(j2\pi f)$ at $f = f_o$ is as close as possible to 1.

The curve of fig. 3-4 shows the polar diagram of the equation 21 as function of f/f_o with

$$n = 1\ ,\quad \frac{f_o}{f_m} = 0.5\ ,\quad \zeta = 0.6\ ,\quad C = 0{,}93 \qquad (22)$$

"A" is then given by

$$A = C\sqrt{1-2(1-2\zeta^2)(\frac{f_o}{f_m})^2 + (\frac{f_o}{f_m})^4}^{1/2} = 0.94 \qquad (23)$$

Curve No. 2 of fig. 3-5 is the polar diagram of the open loop frequency response $K(j2\pi f)$ at f_o = 0.02 c.p.s. in the case in which $m(j2\pi f)$ is defined by eqs. 21 and 22. The system also in this case is stable and the gain at $f = f_o$ has become about 50, which means a precision of about 2%.

A quantity, which may be of interest to the designer, is the angle "α" (fig. 3-5) between the axis, which joins the working point ($f=f_o$=0.02 c.p.s.) to the origin, and the tangent to the big lobe. We have approximately

$$\alpha \simeq \text{arctg} \frac{|M(j2\pi f_o)|}{\sqrt{1-|M(j2\pi f_o)|^2}} = \frac{C}{\sqrt{1-C^2}} \qquad (24)$$

When $C \to 1$, the working point goes to infinite and "α" tends to 90°.

4. Results of the studies on the analog computer

The performance of the automatic control system connected to the Sefor plant to perform the B.O.T.'s has been investigated on the analog computer. The Sefor model was simulated on the computer, and the H.G.U. consisted of a memory with a paper tape punching and reading unit with associated adjustable electronic filter.

The investigation was carried out over the complete range of frequencies at which the 1st and the 2nd B.O.T. will be performed on Sefor typical examples of the results as given in fig. 4-1 and 4-2.

Fig. 4-1 refers to the 1st B.O.T.. The frequency of the experiment was 0.01 c.p.s.

The diagram shows the behaviour of the outlet temperature signal.

Up to the point "A" the reactivity signal was not compensated and the pump was running at constant speed.

At the point "A" the feedback becomes effective, but the H.G.U. is still disconnected. The amplitude of the temperature oscillation is reduced, due to the

compensating signal which feeds the pump.

At the point "B" the H.G.U. was connected.

The effect of the H.G.U. began to appear one period later and the amplitude of the coolant outlet temperature oscillations was progressively reduced to 1/50 of its initial value in about 3 periods (fig. 4-1).

Fig. 4-2 refers to the 2nd BOE at the frequency 0.02 c.p.s.

The diagram shows the behaviour of the power: the final amplitude is of the order 1/100 of its initial value and it is reached in approximately 8 periods.

The flux signal (which was not filtered through a large time constant as it was in the case of the coolant outlet temperature signal that is filtered through the thermal time constants) gave the opportunity to test the performance of the system under severe noise conditions. Under these conditions the measurement of the power oscillations had to be performed with the help of a Transfer Function Analyzer.

As a general result, it can be stated that the study on the analog computer have been in complete agreement with the analytical study of the system.

5. Practical realisation of the system

The system will consist basically (fig. 5-1) of an "input section" on "high gain unit section" and on output section.

5.1 Input section

The input section allows the connection of the system to the signal of the coolant temperature open across the core as required for the 1st B.O.T., or to the flux signal as required for the 2nd B.O.T., and provides the necessary amplification. The D.C. component of the input signal is suppressed by means of a summing unit and of a reference voltage source.

5.2 High Gain Unit (H.G.U.)

The "High Gain Unit" consists basically of an operational amplifier with a positive feedback loop.

The positive feedback loop must be able to pick-up the output signal from the

amplifier and feed it back into the amplifier with a delay "T_o" equal to the oscillation period of the disturbance. The delay is produced with a memory.

The selected memory is a complete punching-reading paper tape unit consisting of the following components:

Control Unit
Analog to digital converter
Puncher encoder
Puncher
Tape
Reader
Encoder
Digital to analog converter

The output signal from the amplifier is sampled once every degree of the oscillation cycle and is stored on the tape in digital form. In order to guarantee the synchronization between the memory and the disturbance oscillation, a pulse generator, giving a pulse for each degree of rotation, will be mounted on the mechanism which produces the disturbance in the plant (for example on the control rod oscillator). These pulses will trigger the memory.

The length of the tape, or better the number of words on the tape between puncher and reader, determines the delay time of the memory.

The gain of the positive feedback loop must be as close as possible to 1, but never greater than 1. Since the positive feedback loop contains a low pass filter to improve stability, the length of the tape between puncher and reader must not give a delay equal to "T_o", but a delay "T_o^*" equal to:

$$T_o^* = T_o \left(1 - \frac{\phi_o}{2\pi}\right) \qquad (1)$$

where ϕ_o is the phase shift introduced by the filter at the working frequency "f_o" = $1/T_o$. The filter is of an adjustable electronic type, consisting of four sections used in the low pass mode.

5.3 Output section

The output signal from the "High Gain Unit" will be fed into an adopting component in order to meet the input requirements of the "Primary Pump Control Circuit".

5.4 Safety features

The safety features consist of two trip amplifiers that will monitor the input and the output signals of the automatic control system. If either one of these signals exceed a preset level, the corresponding trip amplifier will disconnect the automatic control system from the primary pump control circuit.

5.5 Detailed design

The detailed design of the system is given in fig. 5-2.

This figure shows the amplifiers and the potentiometers necessary for the precise adjustment of the gain, and the instrumentation to monitor the performances of the system. A picture of the panels containing the equipment for the automatic control system is given in fig. 5-3.

6. Final Considerations

The type of Automatic Control System, which has been described in the preceeding paragraphs, has the following characteristics.

1. It allows to reach a very high precision at the frequency "f_o" of the experiment. This is obtained by setting the gain of the H.G.U. at f_o as near as possible to 1 and the phase delay "ψ" of the memory in such a way that:

$$\psi + \phi_o = 2\pi \qquad (1)$$

where ϕ_o ist the phase shift of the L.P.F. at the frequency "f_o". The precision is limited by the practical limitations of carrying out these two settings. "C" can be set within ± 1%. If we choose for "C" the value 0,98 the open loop gain will be 50 and therefore the error "E" is 2% i.e. the oscillation of the controlled variable at frequency "f_o" will be reduced to 2% of the disturbance. This is valid if the phase is supposed to be set perfectly. Fig. 6.1 shows the error "E" as function of the difference "$\delta\psi$" between the setted value of ψ and its corrected value (see Appendix 2). It appears that "E" is sensitive to this phase setting error "$\delta\psi$". The memory has a paper tape which moves under the writing and the reading heads. The tape has a line of holes and the distance between hole and hole will correspond to an angle of 1 degree. In this way 360°

will be given by 360 holes. The value of ψ is set by choosing the right length of the tape between the two heads that is by counting the right number of holes. The system is by itself capable to have a sensitivity of ± 0.5 degree. The precision in setting "ψ" will therefore depend upon the way in which the calibration of memory plus filter is carried out. The reproducibility of the setting of ψ is very good.

2. The open loop gain drops as the frequency moves a little from the selected frequency "f_o". The synchronization between the tape speed and the frequency "f_o" is therefore required. The movement of the tape must be derived by the "Frequency and Sinus Function Generator" shown in the schemes of figs. 2-1A, 2-1B, 2-2A and 2-2B.

3. The system is capable to provide an high open loop gain at very low frequences (figs. 3-2 and 3-5) which means that it can cope with the drift of the plant.

   The time needed by the system to reach the balance condition, that is to compensate for the disturbances U_1 (fig. 3-1), can be approximately estimated as follows. We can say that at the "n"th cycle the oscillation amplitude of the controlled variable U will be reduced approximately by a factor (Appendix 1).

$$\frac{C^{n-1}}{|1+W(j2\pi f_o)|^n} + \frac{1-C}{|1+W(j2\pi f_o)|} \cdot \frac{1-\underline{/}\bar{C}/|1+W(j2\pi f_o)|\underline{/}^{(n-1)}}{1-C/|1+W(j2\pi f_o)|} \qquad (2)$$

   In the case shown in fig. 3-5 we have

$$C = 0.98 \qquad (3)$$

   and

$$|1+W(j2\pi\ 0.02)| = 1.35 \qquad (4)$$

   This means that the amplitude of the controlled signal will be reduced in 6 cycles to about 4.5 % of its initial value.

   Looking at fig. 3-5 we see that the modulus of the functions $K(j2\pi f)$ and $W(j2\pi f)$ can be increased by a factor of 1.5 without having problems with stability. If this is done, the numerical value of eq. 4 becomes 2.4 instead of 1.35, and the same reduction of amplitude will be reached in only 4 cycles.

4. It is very interesting to notice that, after few cycles, the memory has already instored the right corrective signal, so that the control loop can even be open while the tape continues to feed the plant with the right corrective signal. In this case it is more convenient to have a second

reading head (at 360° from writing head) which gives the signal to the writing head in such a way, that the signal remains in the tape always unchanged. The first reading head will continue to feed the plant. This feature seems valuable, if one thinks to repeat a B.O.T.. In this case the right corrective signal already exists instored in the tape, which can feed the plant directly. An additional control loop, able to cope only with the drift of the plant, could be added to the system. For a better precision it would be convenient to have this second loop working in parallel to the tape also when the tape is recording the corrective signal.

Appendix 1

Approximate Evaluation of the Behaviour of the Controlled Variable in the Time Dom

Let us consider the closed loop control system of fig. 3-1.

We write eq. 11 of para. 3

$$\frac{U}{U_1} = \frac{1}{1+K(s)} \tag{1}$$

where

$$K(s) = W(s)\ \frac{1}{1-M(s)} \tag{2}$$

and

$$W(s) = P_2(s)\ H(s)\ G(s) \tag{3}$$

We suppose that $U_1(t)$ is a sinusoidal function in the time domain. We have

$$U_1(t) = U_o \sin 2\pi f_o t \tag{4}$$

In the Laplace domain we have

$$U_1 = U_o\ \frac{2 f_o \pi}{s^2+(2\pi f_o)^2} \tag{5}$$

Eq. 1 becomes

$$U = U_o\ \frac{2\pi f_o}{s^2+(2\pi f_o)^2}\ \frac{1}{1+W(s)\ \frac{1}{1-M(s)}} \tag{6}$$

From eq. 6 in the time domain we get

$$U(t) = U_o L^{-1} \left\{ \frac{2\pi f_o}{s^2+(2\pi f_o)^2}\ \frac{1}{1+W(s)\ \frac{1}{1-M(s)}} \right\} \tag{7}$$

Where the symbol L^{-1} indicates antitransformation.

We shall solve eq. 7 in the case

$$M(s) = AF(s)\quad \exp.\ (-\psi s/2\pi f_o) \tag{8}$$

where F(s) is the transfer function of the L.P.F.

Taking into account eq. 8, eq. 6 becomes

$$U = U_o \frac{2\pi f_o}{s^2+(2\pi f_o)^2} \frac{1}{1+W(s)} \frac{1-AF(s)\exp(-\psi s/2\pi f_o)}{1-[AF(s)\exp(-\psi s/2\pi f_o)]/(1+W(s)} \quad (9)$$

Eq. 9 can be written as follows

$$U = U_o \frac{2\pi f_o}{s^2+(2\pi f_o)^2} [1-AF(s)\exp(-\psi s/2\pi f_o)] \sum_{n=1}^{\infty} (-1)^n \frac{[AF(s)]^{n-1}}{[1+W(s)]^n} \exp[-(n-1)\frac{\psi s}{2\pi f_o}] \quad (10)$$

$$U = U_o \frac{2\pi f_o}{s^2+(2\pi f_o)^2} \sum_{n=1}^{\infty} (-1)^{n-1} \frac{[AF(s)]^{n-1}}{[1+W(s)]^n} \exp[-(n-1)\frac{\psi s}{2\pi f_o}]-AF(s)\exp(-n\frac{\psi s}{2\pi f_o}) \quad (11)$$

We shall antitransform eq. 11 in the particular case

$$AF(s) = A \quad (12)$$

$$W(s) = W_o = \text{const.} \quad (13)$$

$$\psi = 2\pi \quad (14)$$

Taking into account eqs. 12, 13 and 14, eq. 11 becomes

$$U = U_o \frac{2\pi f_o}{s^2+(2\pi f_o)^2} \sum_{n=1}^{\infty} (-1)^{n-1} \frac{A^{n-1}}{(1+W_o)^n} [\exp[-(n-1)\frac{s}{f_o}] - A \exp(-n\frac{s}{f_o})] \quad (15)$$

The antitransform of eq. 15 is:

$$U(t) = U_o \sin(2\pi f_o t) \sum_{n=1}^{\infty} \frac{A^{n-1}}{(1+W_o)^n} [1(t-\frac{n-1}{f_o})-A\cdot 1(6-\frac{n}{f_o})] \quad (16)$$

where

n = "n"th oscillation

and 1(t) indicates step function.

Eq. 16 is shown in fig. A1-1. The controlled variable U(t) oscillates with an amplitude which is decreasing with the time and taking the following values

1st oscillation $U_o \frac{1}{1+W_o}$ (17)

2nd oscillation $U_o \left\{\frac{A}{(1+W_o)^2} + \frac{1-A}{1+W_o}\right\}$ (18)

$$\text{"n"th oscillation} \quad U_o \left\{ \frac{A^{(n-1)}}{(1+W_o)^n} + \frac{1-A}{1+W_o} \; \frac{1-\underline{/\bar{A}/(1+W_o)}\underline{/}^{(n-1)}}{1-A/(1+W_o)} \right\} \tag{19}$$

After a large number of oscillations ($n \to \infty$), the amplitude of the controlled variable will tend to the asymptotic value.

$$U_o \frac{1-A}{1+W_o} \; \frac{1}{1-A/(1+W_o)} = U_o \frac{1}{1+\frac{W_o}{1-A}} \tag{20}$$

Eq. 19 suggests an approximate expression for the evaluation of the amplitude of the controlled variable at the "n"th oscillation.
If we substitute eqs. 12, 13 and 14 respectively with

$$\underline{AF(s)} = A\underline{|F(j2\pi f_o)|}\underline{\exp(-j\phi_o \frac{s}{2\pi})} = C \exp(-j\phi_o \frac{s}{2\pi}) \tag{21}$$

$$W(s) = W(j2\pi f_o) \tag{22}$$

and

$$\psi = 2\pi - \phi_o \tag{23}$$

and with these new values we antitransform eq. 11, we get at the "n"th oscillation the following expression for the amplitude of the controlled variable U

$$U_o \left\{ \frac{C^{n-1}}{|1+W(j2\pi f_o)|^n} + \frac{1-C}{|1+W(j2\pi f_o)|} \; \frac{1-\underline{/\bar{C}/|1+W(j2\pi f_o)|}\underline{/}^{(n-1)}}{1-C/|1+W(j2\pi f_o)|} \right\} \tag{24}$$

Appendix 2

Dependence of the precision upon the error "$\delta\psi$" of phase setting

The error "E" of the controlled variable "U" is given by (eq. 11 of para. 3)

$$E = \left|\frac{U}{U_1}\right| = \left|\frac{1}{1+K(j2\pi f_o)}\right| \simeq \left|\frac{1}{K(j2\pi f_o)}\right| = \left|\frac{1}{W(j2\pi f_o)}\right| \cdot \left|1-Ce^{j\delta\psi}\right| \qquad (1)$$

where C is defined by eq. 23 of para. 3.

Eq. 1 can be written as follows

$$E = \left|\frac{1}{W(j2\pi f_o)}\right| \cdot \left|1-C\cos\delta\psi + j\,C\sin\delta\psi\right| = \left|\frac{1}{W(j2\pi f_o)}\right| \sqrt{(1-C\cos\delta\psi)^2+(C\sin\delta\psi)^2} \qquad (2)$$

Since

$$\cos\delta\psi \simeq 1 \qquad (3)$$

and

$$\sin\delta\psi \simeq \delta\psi \qquad (4)$$

eq. 2 becomes

$$E \simeq \frac{1-C}{|W(j2\pi f_o)|}\sqrt{1+\left(\frac{C}{1-C}\,\delta\psi\right)^2} \qquad (5)$$

Fig. 6-1 shows the ratio

$$\frac{E}{E_{id}} = \frac{E|W(j2\pi f_o)|}{1-C} = \sqrt{1+\left(\frac{C}{1-C}\,\delta\psi\right)^2} \qquad (6)$$

as function of "$\delta\psi$" for different values of "C". "E_{id}" is given by

$$E_{id} = \frac{1-C}{|W(j2\pi f_o)|} \qquad (7)$$

References

1. L. Caldarola: The Balanced Oscillator Experiment
Nukleonik, Band 7, Heft 3, 1965, S. 120-127

2. L. Caldarola and C. Russell: The Second Balanced Oscillator Experiment
Nukleonik, Band 9, Heft 7, 1967, S. 323-329

3. R. Pflasterer and L. Caldarola: SEFOR Task 1.1
Topical Report vol II Test Descriptions General Electric Co. No. GEAP 5092

4. SEFOR Research and Development Program
Third Quarterly Progress Report Oct. 1964-Jan. 1965
General Electric Co. Report No. GEAP 5092

5. L. Noble, G.R.Pflasterer, C.G.Wilkinson and L. Caldarola:
Recent Developments in the SEFOR Experimental Program
International Conference on Fast Critical Experiments and their Analysis
Argonne, October 10-13, 1966

6. M. Audoux, L. Caldarola, P. Giordano, H. Rohrbacher and C. Russel:
The Balanced Oscillator Tests in SEFOR
International Conference on Critical Experiments and their Analysis
Argonne, October 10-13, 1966

7. Chestnut Mayer: Servomechanism and Regulating System Design
John Wiley and Sons, New York, 1951

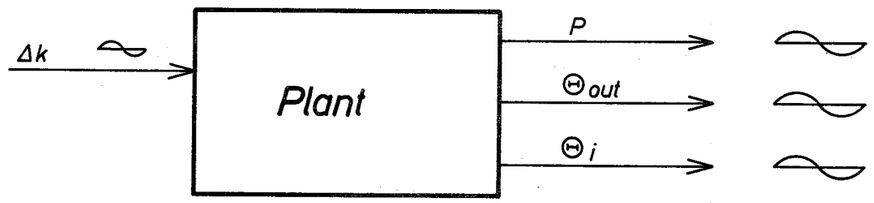

Legend

Δk = Reactivity

P = Power

Θ out = Reactor outlet coolant Temperature

Θ i = Reactor inlet

Fig. 1-1A Traditional Oscillator Test

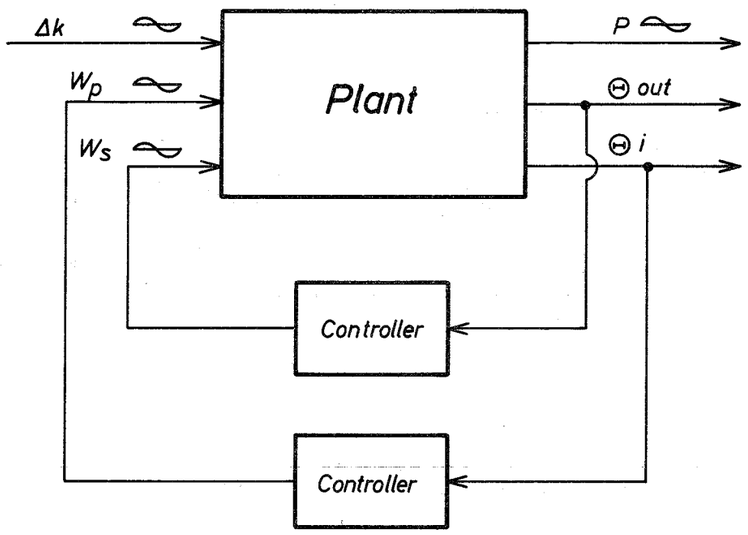

Legend

Δk	=	Reactivity
P	=	Power
Θ out	=	Reactor outlet coolant Temperature
Θ i	=	Reactor inlet coolant Temperature
W_p	=	Primary coolant flow
W_s		Secondary coolant flow

Fig. 1-1B First Balanced Oscillator Test

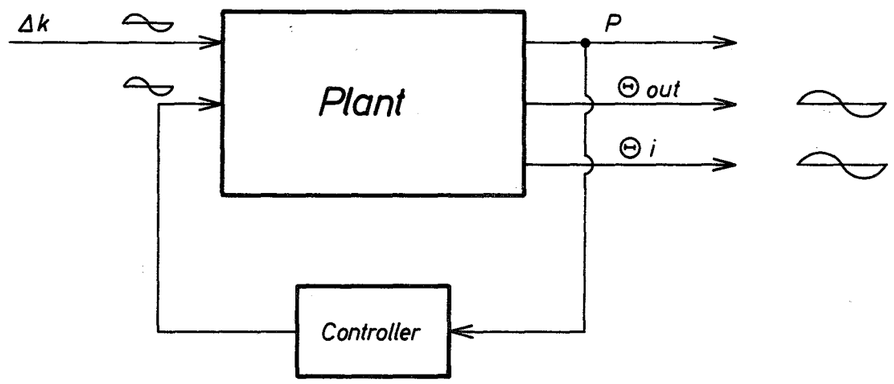

Legend

Δk = Reactivity

P = Power

⊖ out = Reactor outlet coolant Temperature

⊖ i = Reactor inlet coolant Temperature

Fig. 1-1C Second Balanced Oscillator Test

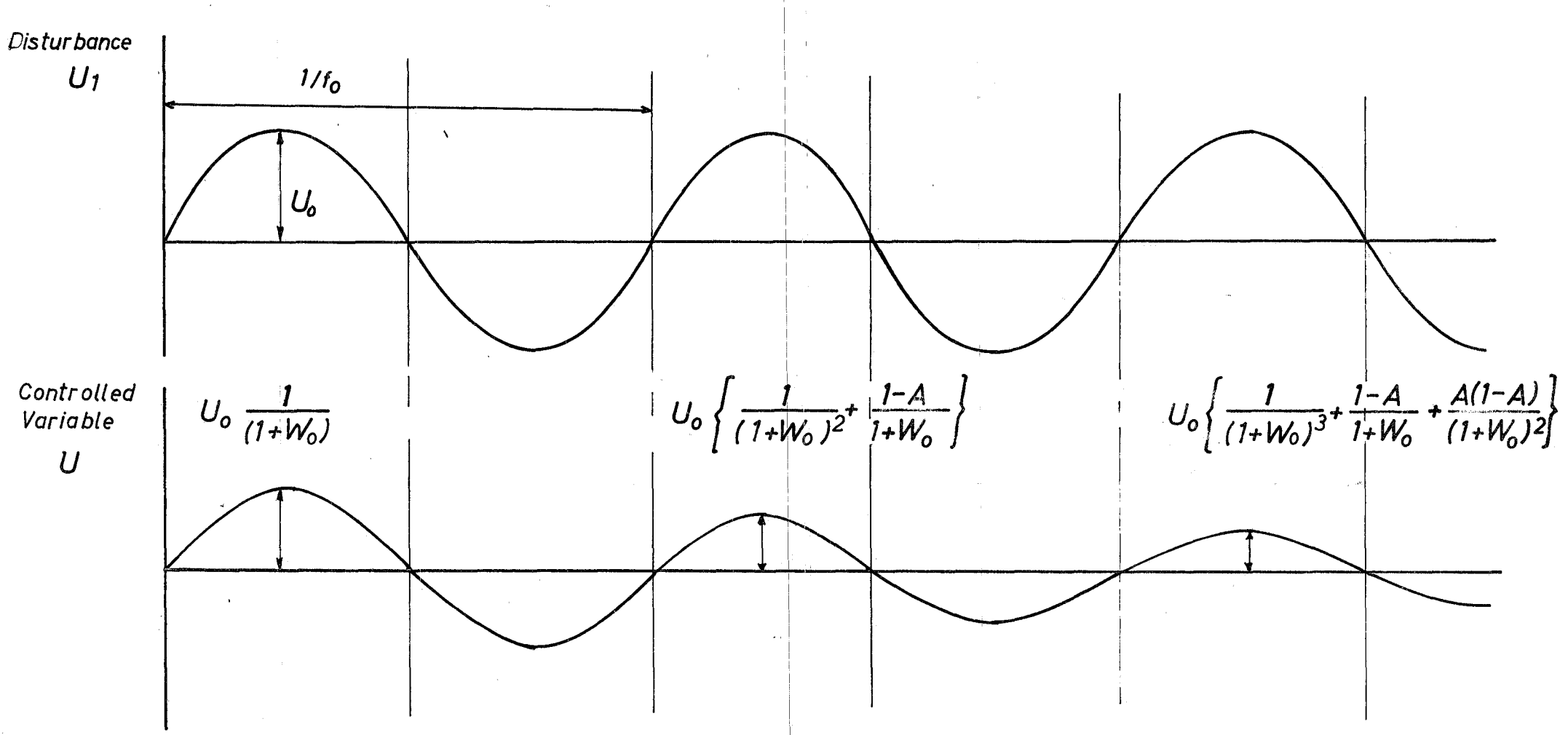

Fig. A1-1 Behaviour of the Controlled Variable U in the ideal case analyzed in Appendix 1

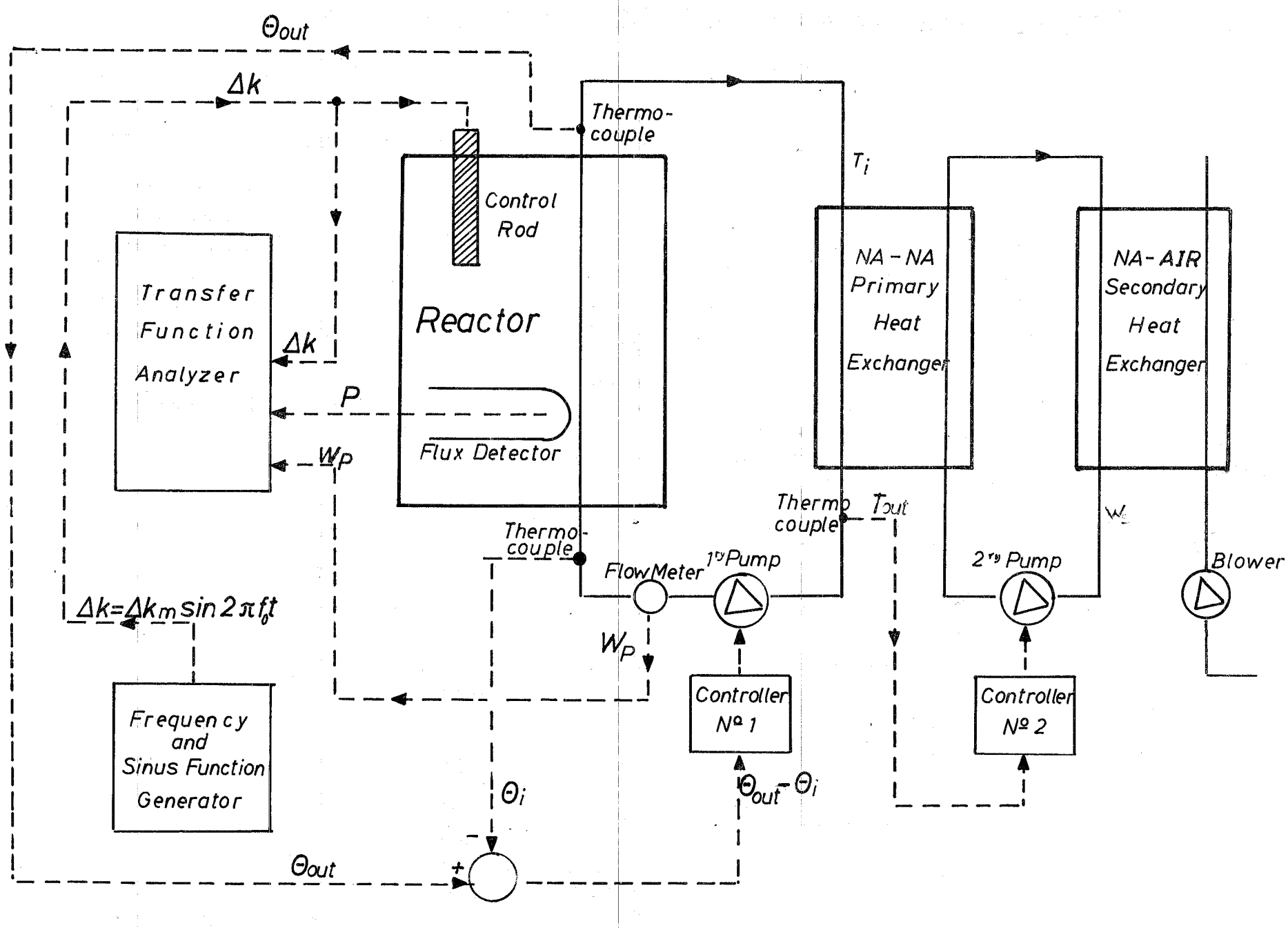

Fig. 2-1A 1st Balanced Oscillator Experiment - Schematic block diagram of the connections of the Closed Loop Control System to the Plant 1st Philosophy Design

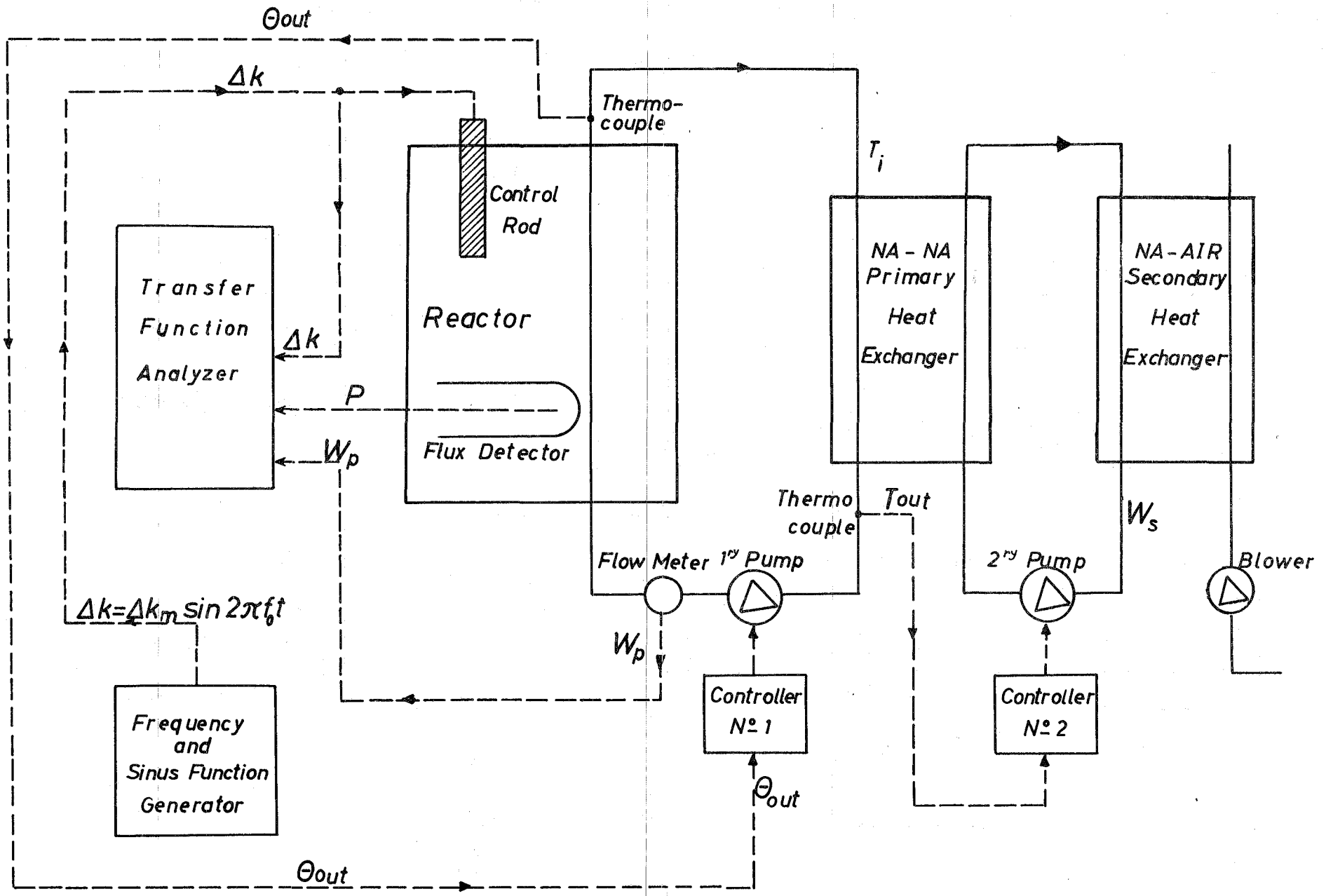

Fig. 2-1B 1st Balanced Osciliator Experiment - Schematic block diagram of the connections of the Closed Loop Control System to the Plant. 2nd Philosophy Design.

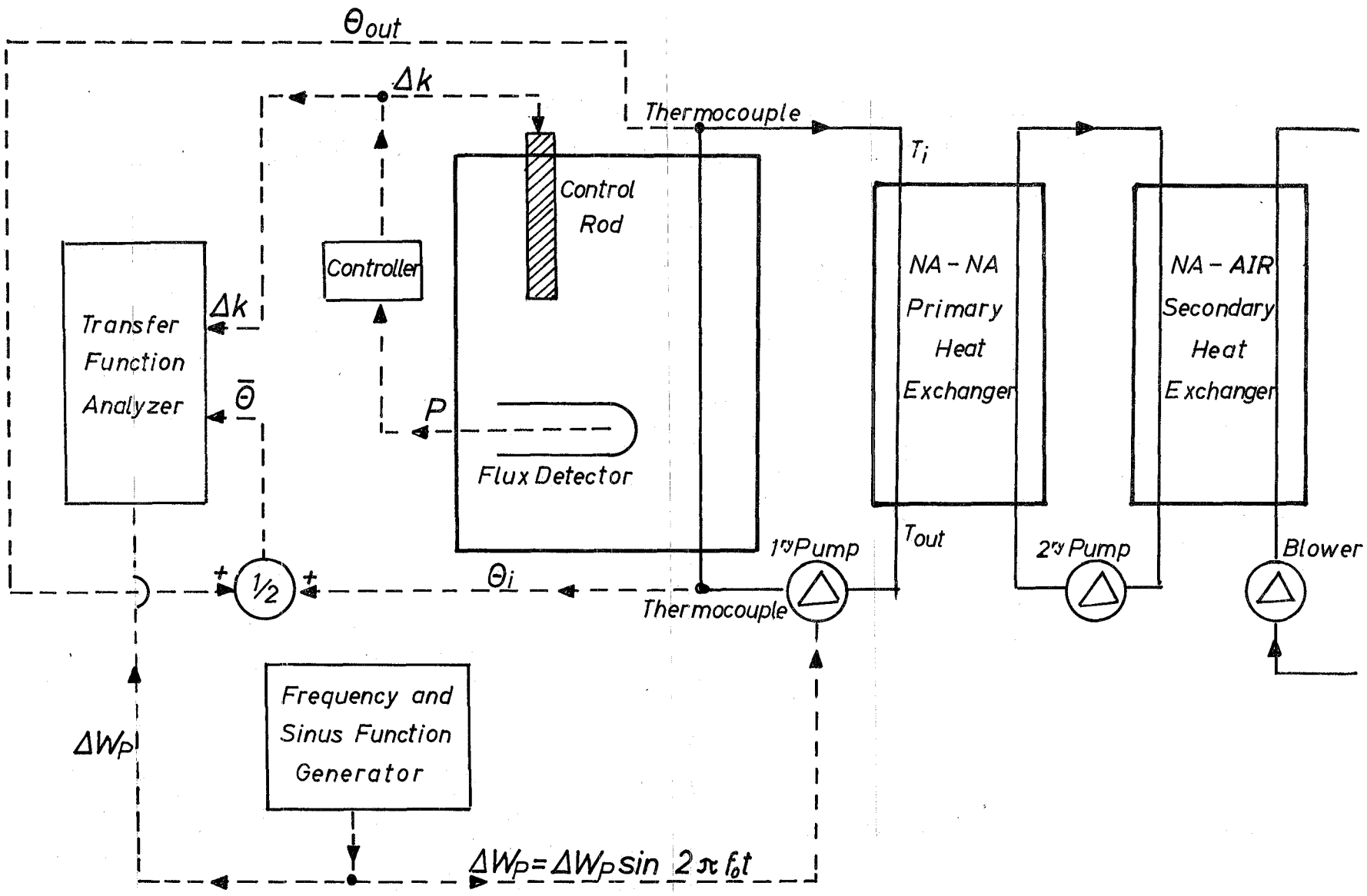

Fig. 2-2A 2nd Balanced Oscillator Experiment -Schematic block diagram of the connections of the Closed Loop Control System to the Plant - 1st Philosophy Design

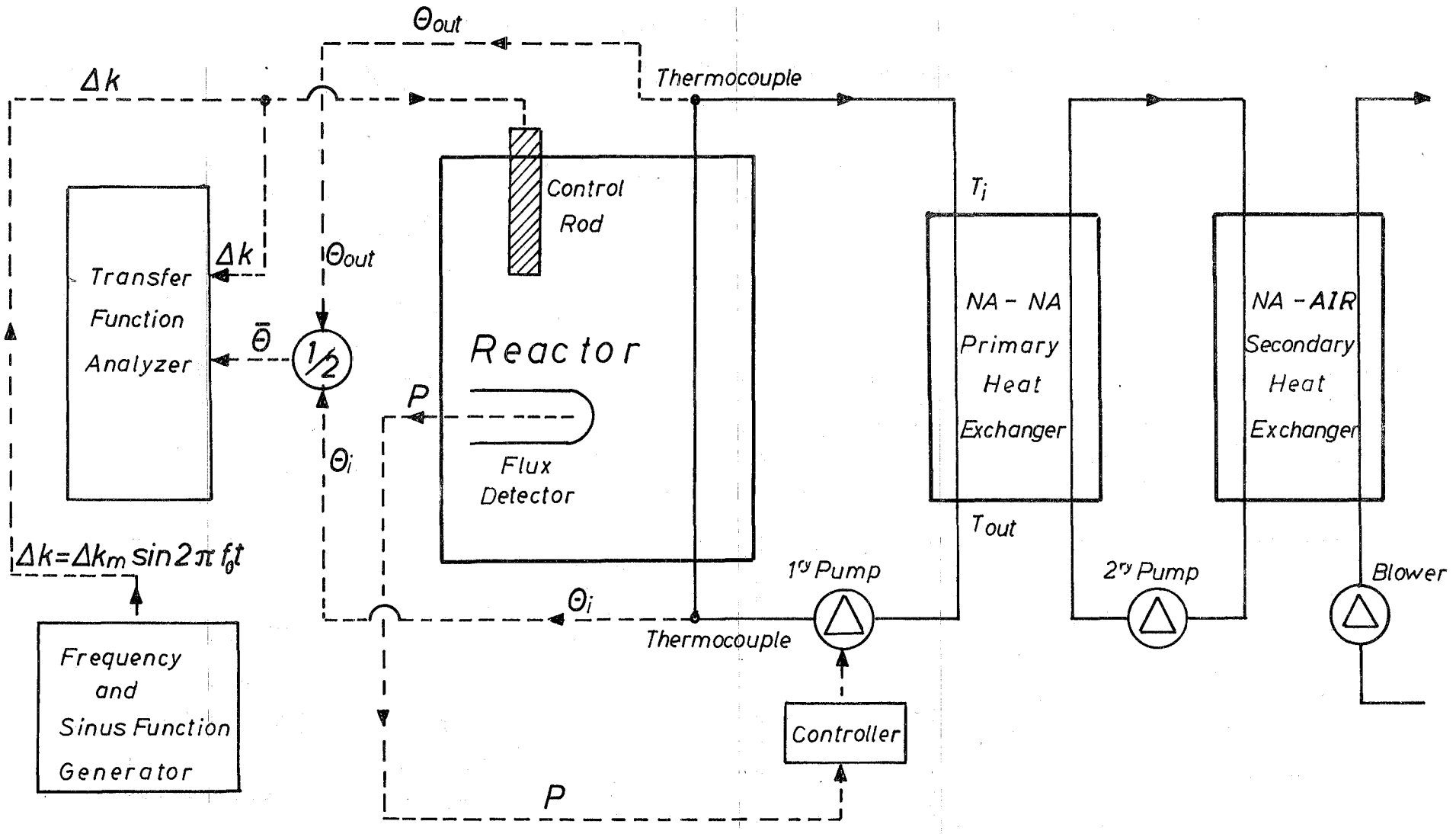

Fig. 2-2B 2nd Balanced Oscillator Experiment – Schematic block diagram of the connections of the Closed Loop Control System to the Plant – 2nd Philosophy Design

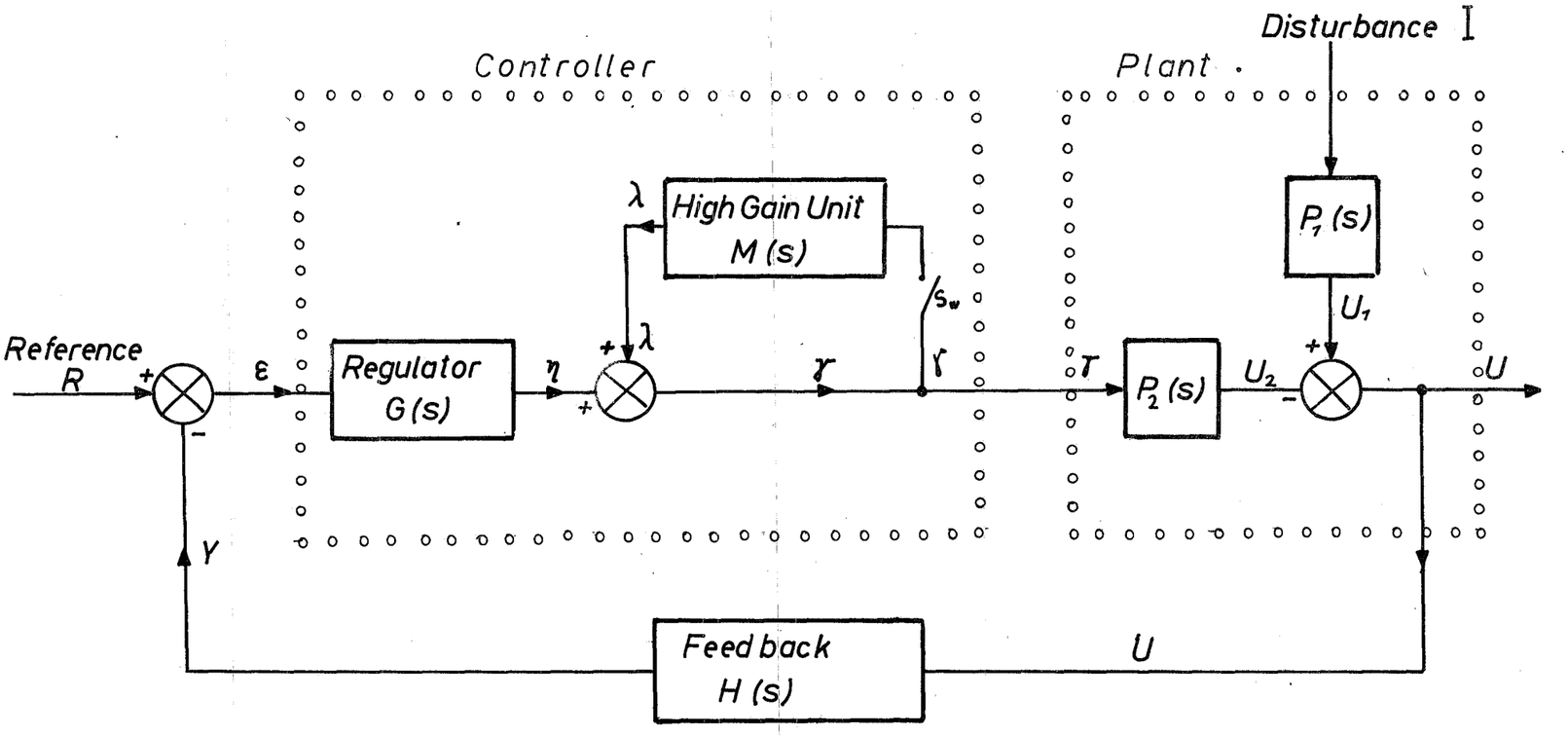

Fig. 3-1 Schematic Block Diagram of the Closed Control Loop

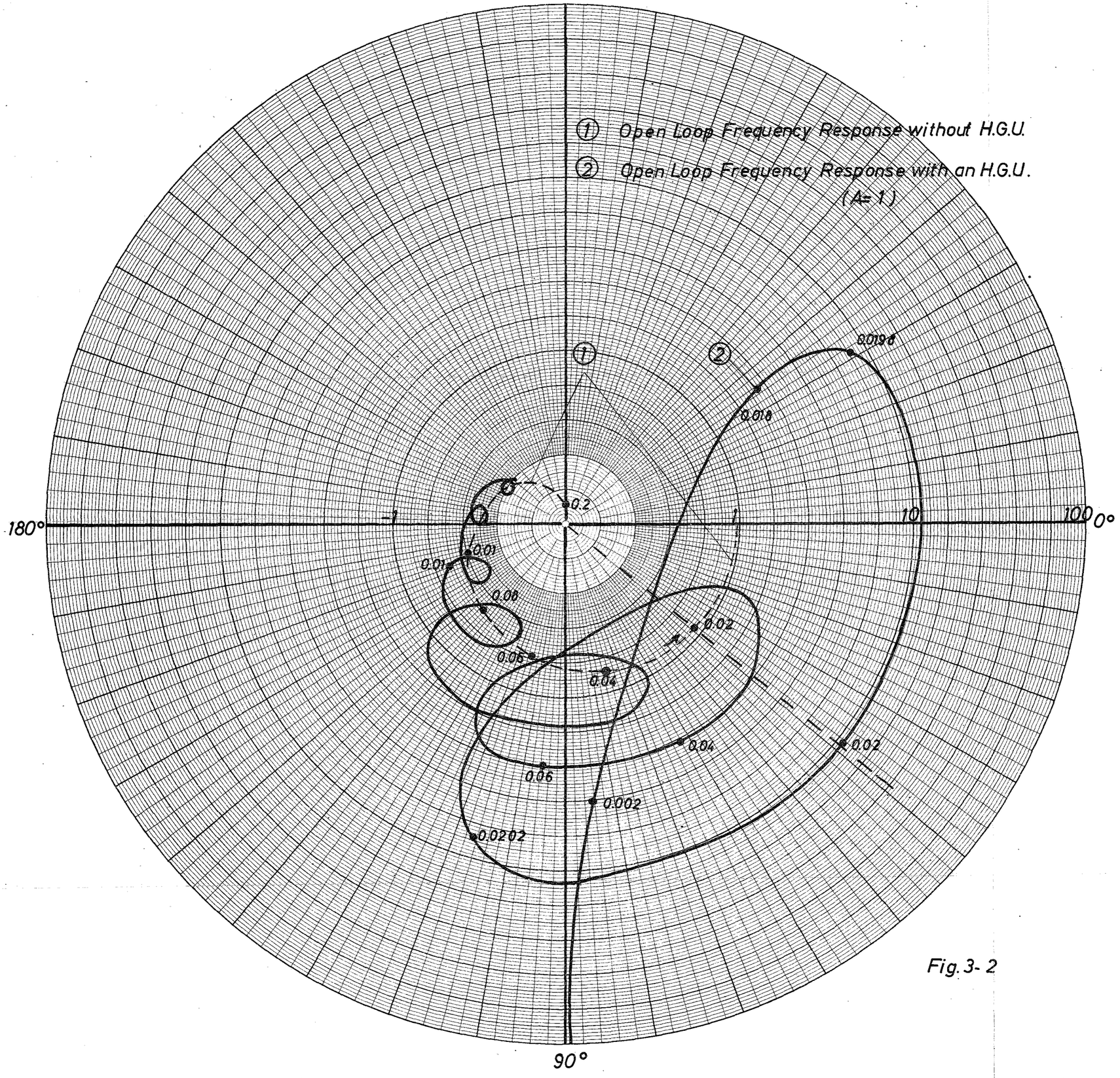
① Open Loop Frequency Response without H.G.U.
② Open Loop Frequency Response with an H.G.U. (A=1)
180°
0°
90°
-1
1
10
100
0.2
0.01
0.01
0.08
0.06
0.04
0.02
0.019 8
0.016
0.04
0.02
0.06
0.002
0.0202

Fig. 3- 2

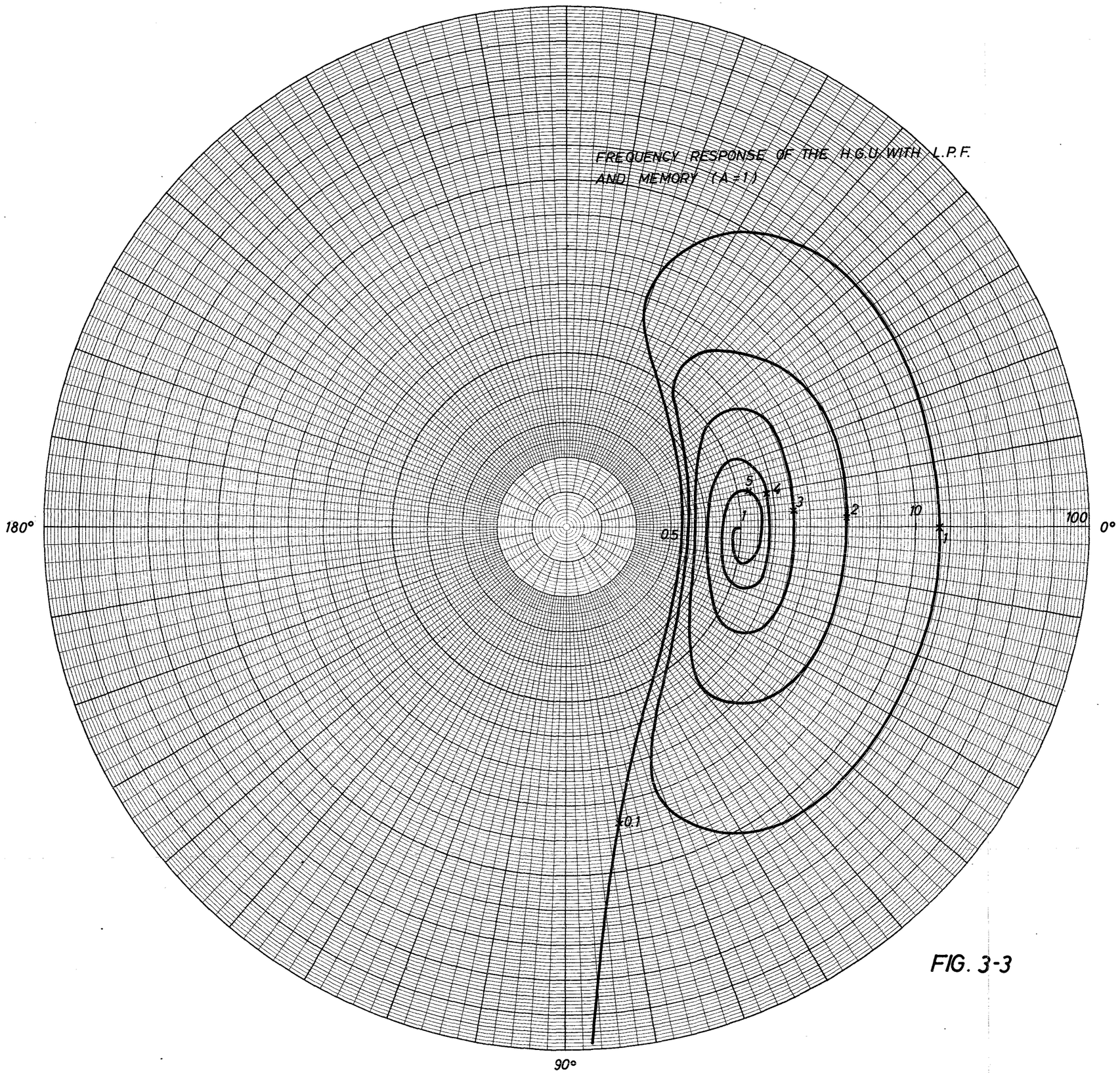
FREQUENCY RESPONSE OF THE H.G.U. WITH L.P.F.
AND MEMORY (A = 1)
180°
0°
90°
0.5
0.1
5
4
3
2
10
1
100

FIG. 3-3

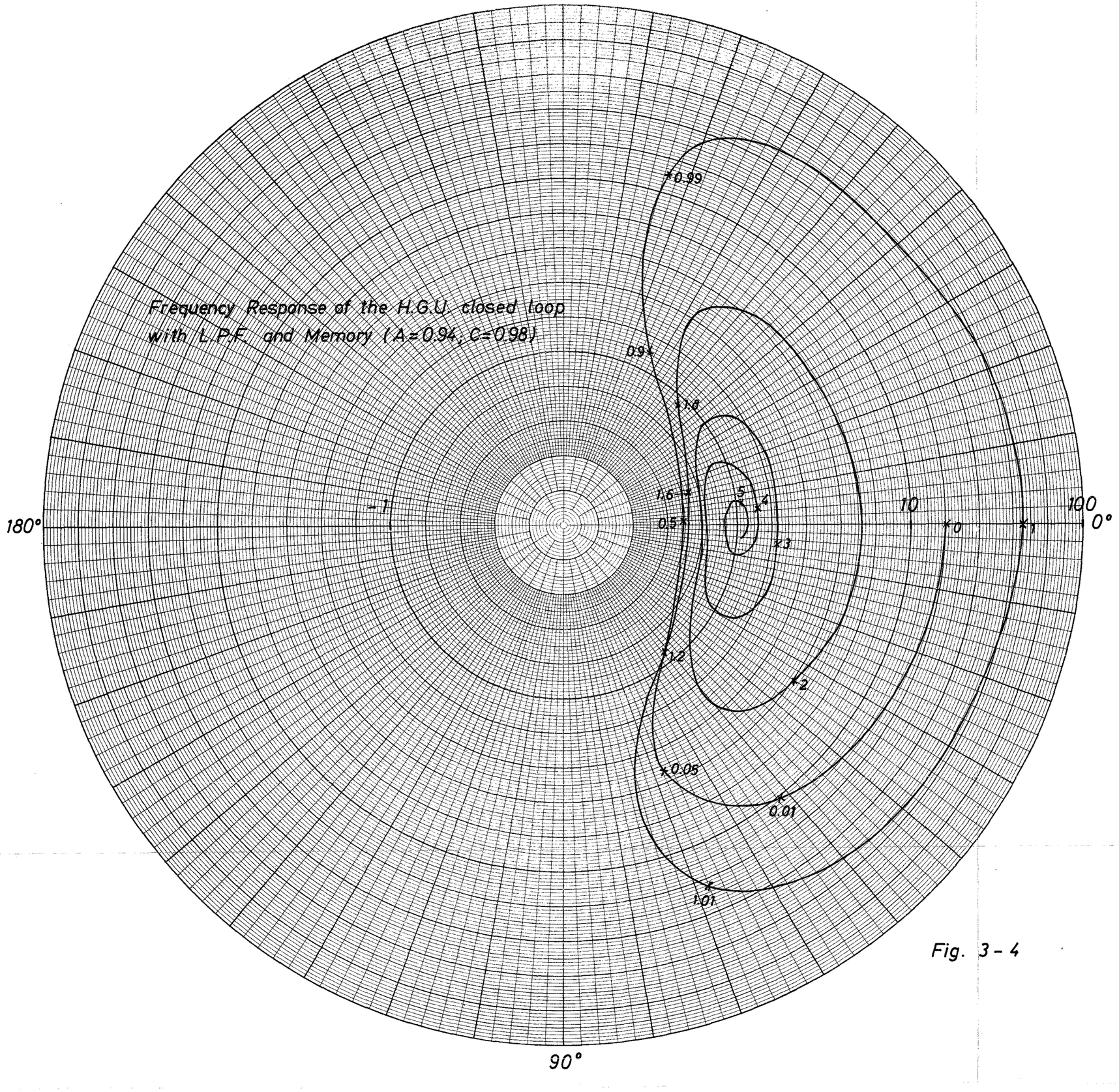
Frequency Response of the H.G.U. closed loop
with L.P.F. and Memory (A=0.94; C=0.98)
180°
90°
0°
-1
10
100
0.99
0.9
1.8
1.6
0.5
5
4
3
1.2
2
0.05
0.01
1.01
0
1

Fig. 3 - 4

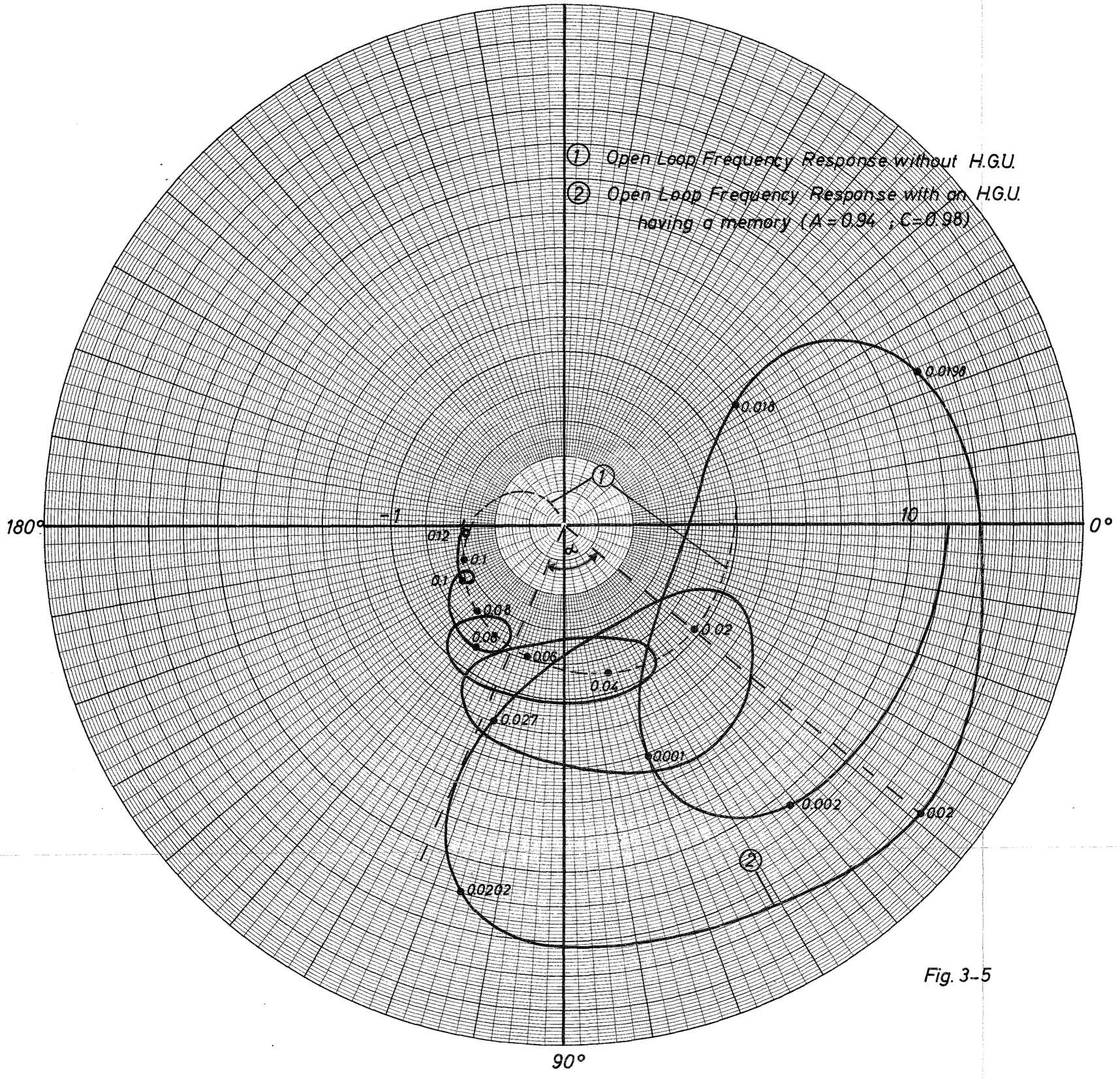
① Open Loop Frequency Response without H.G.U.
② Open Loop Frequency Response with an H.G.U. having a memory (A=0.94 ; C=0.98)
180°
0°
90°
-1
10
ω
0.12
0.1
0.1
0.08
0.06
0.06
0.04
0.02
0.027
0.018
0.0198
0.001
0.002
0.02
0.0202
①
②

Fig. 3-5

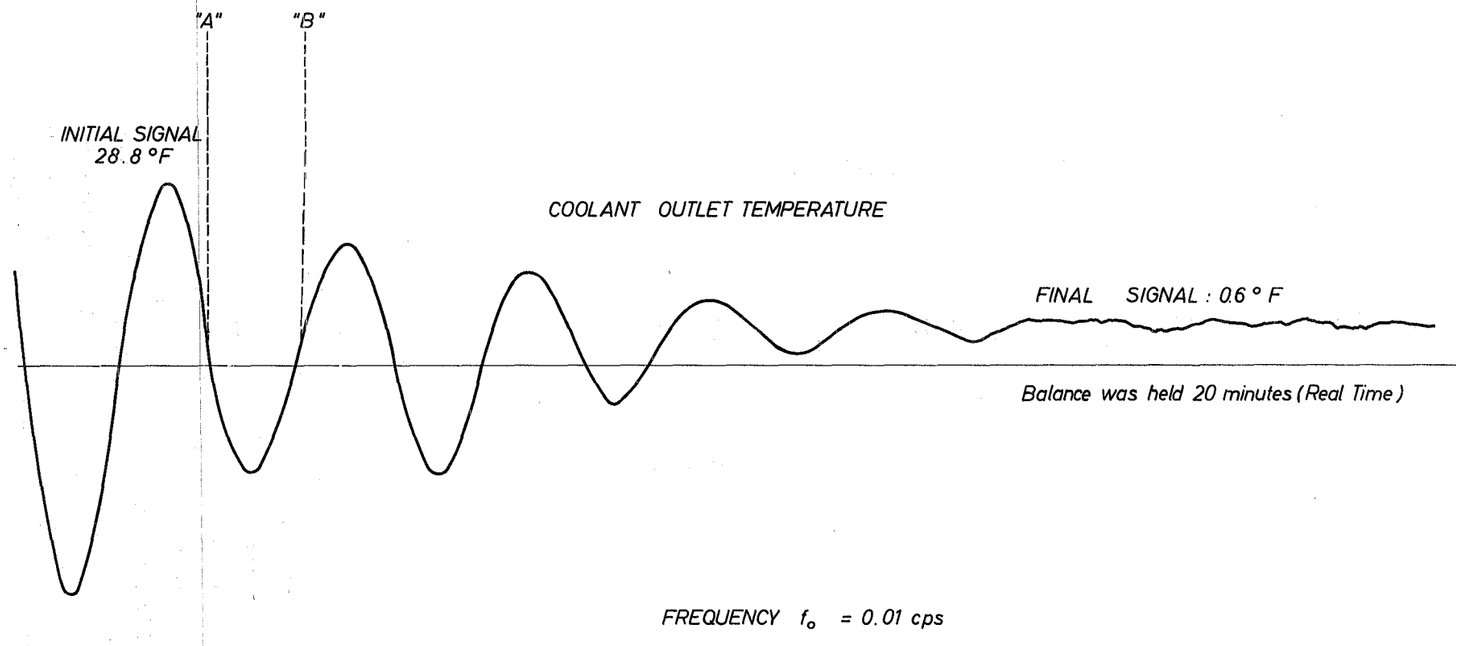
"A"
"B"
INITIAL SIGNAL
28.8 °F
COOLANT OUTLET TEMPERATURE
FINAL SIGNAL : 0.6 ° F
Balance was held 20 minutes (Real Time)
FREQUENCY f_o = 0.01 cps

FIG. 4-1

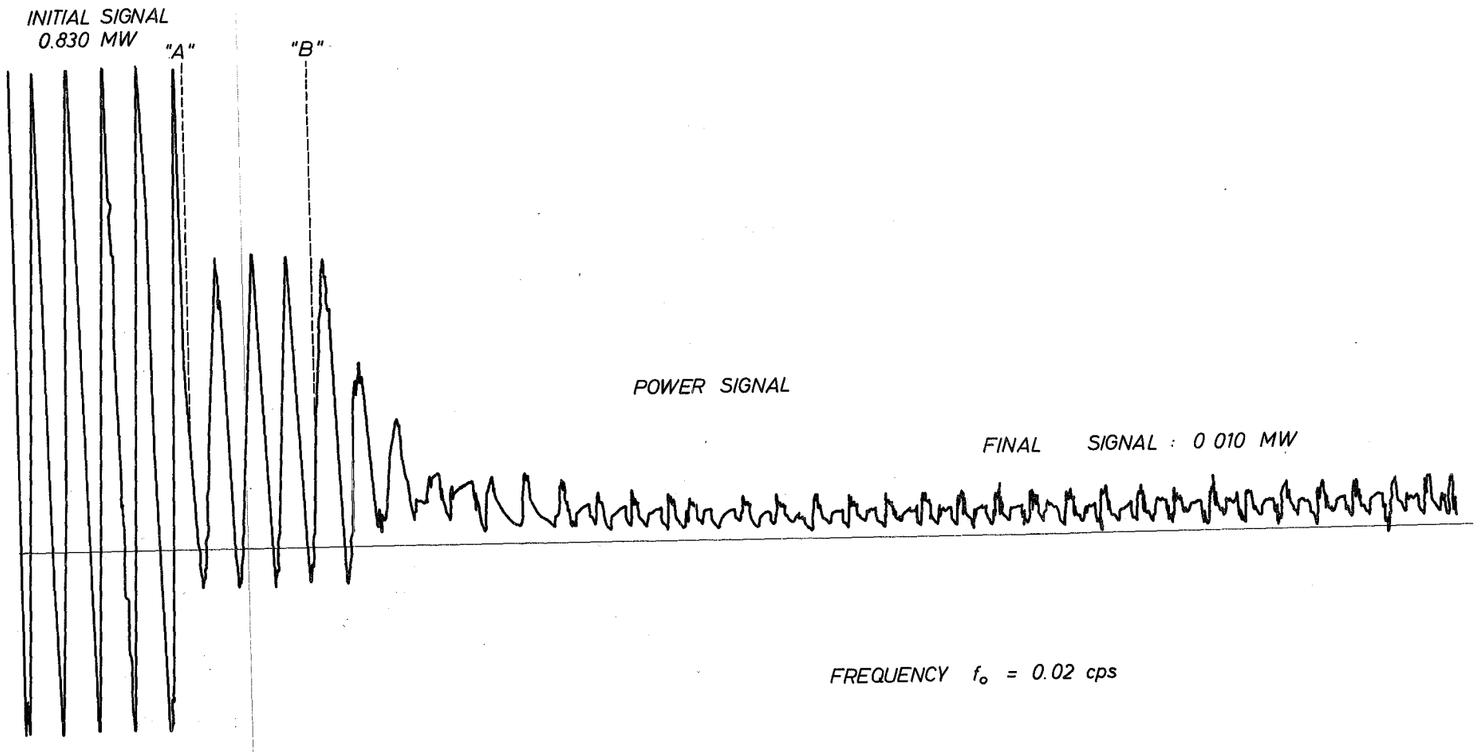
INITIAL SIGNAL
0.830 MW
"A"
"B"
POWER SIGNAL
FINAL SIGNAL : 0 010 MW
FREQUENCY f_o = 0.02 cps

FIG. 4 - 2

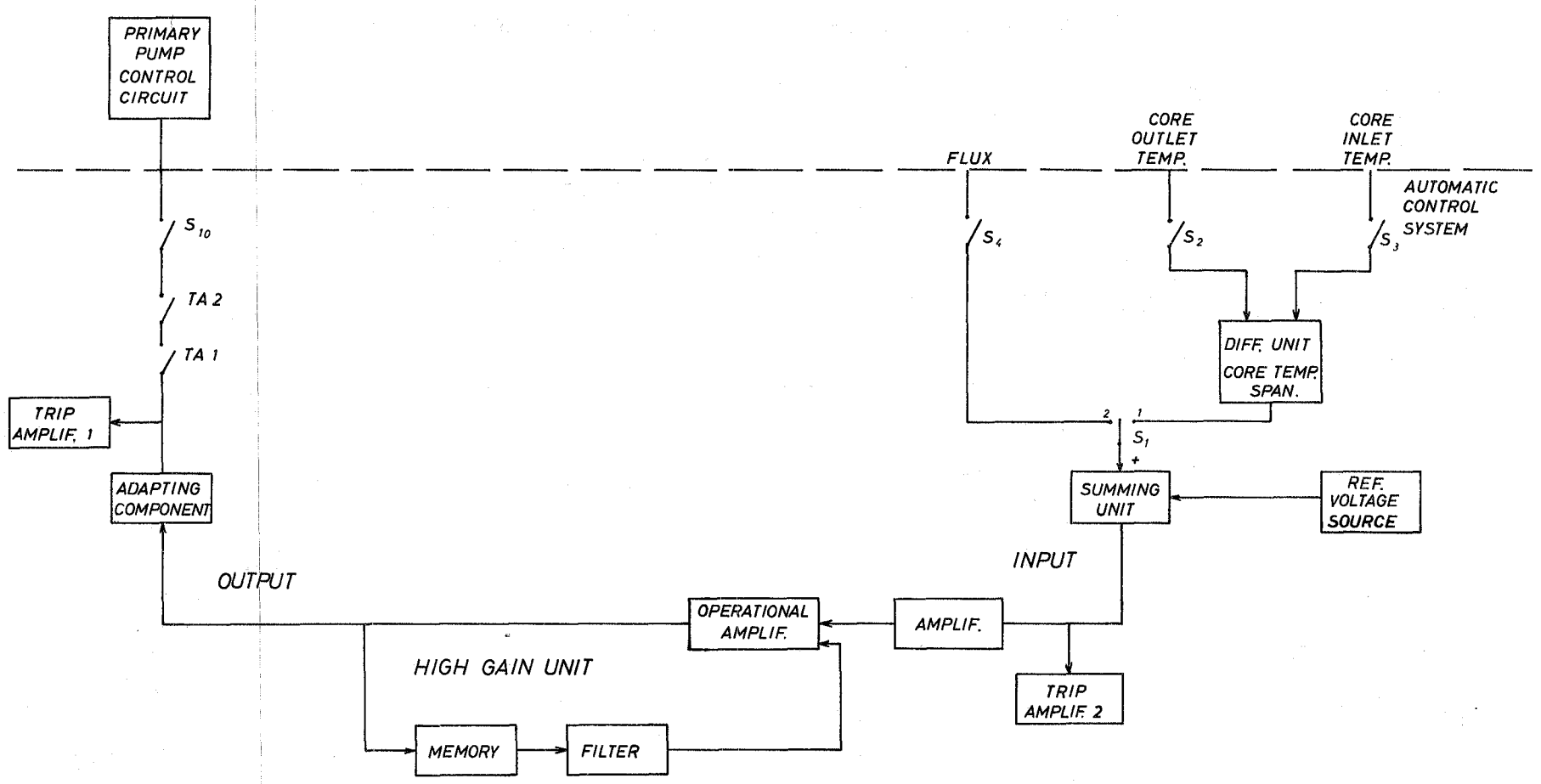

FIG. 5-1 SEFOR PLANT GENERAL LAYOUT OF THE AUTOMATIC CONTROL SYSTEM FOR B.O.E.

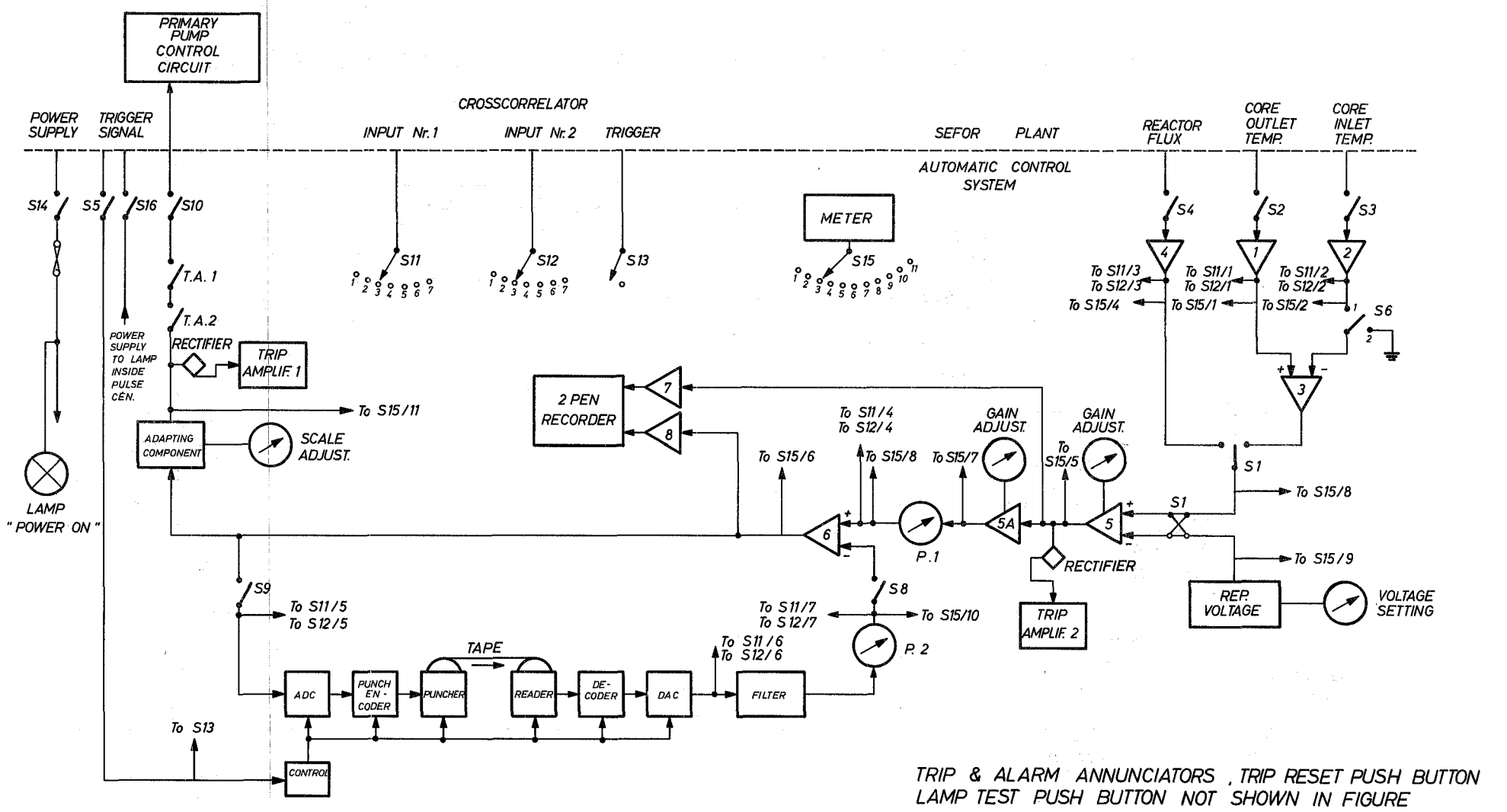

FIG. 5-2 BLOCK DIAGRAMM OF THE AUTOMATIC CONTROL SYSTEM FOR B.O.E.

Figure 5-3

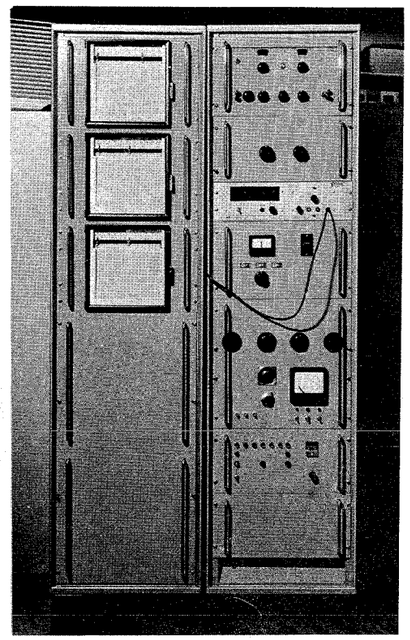

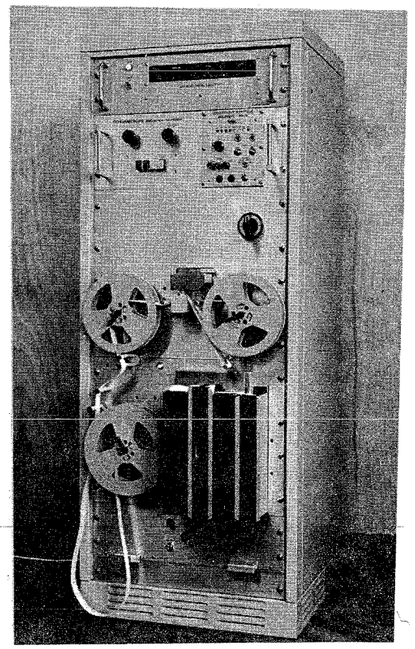

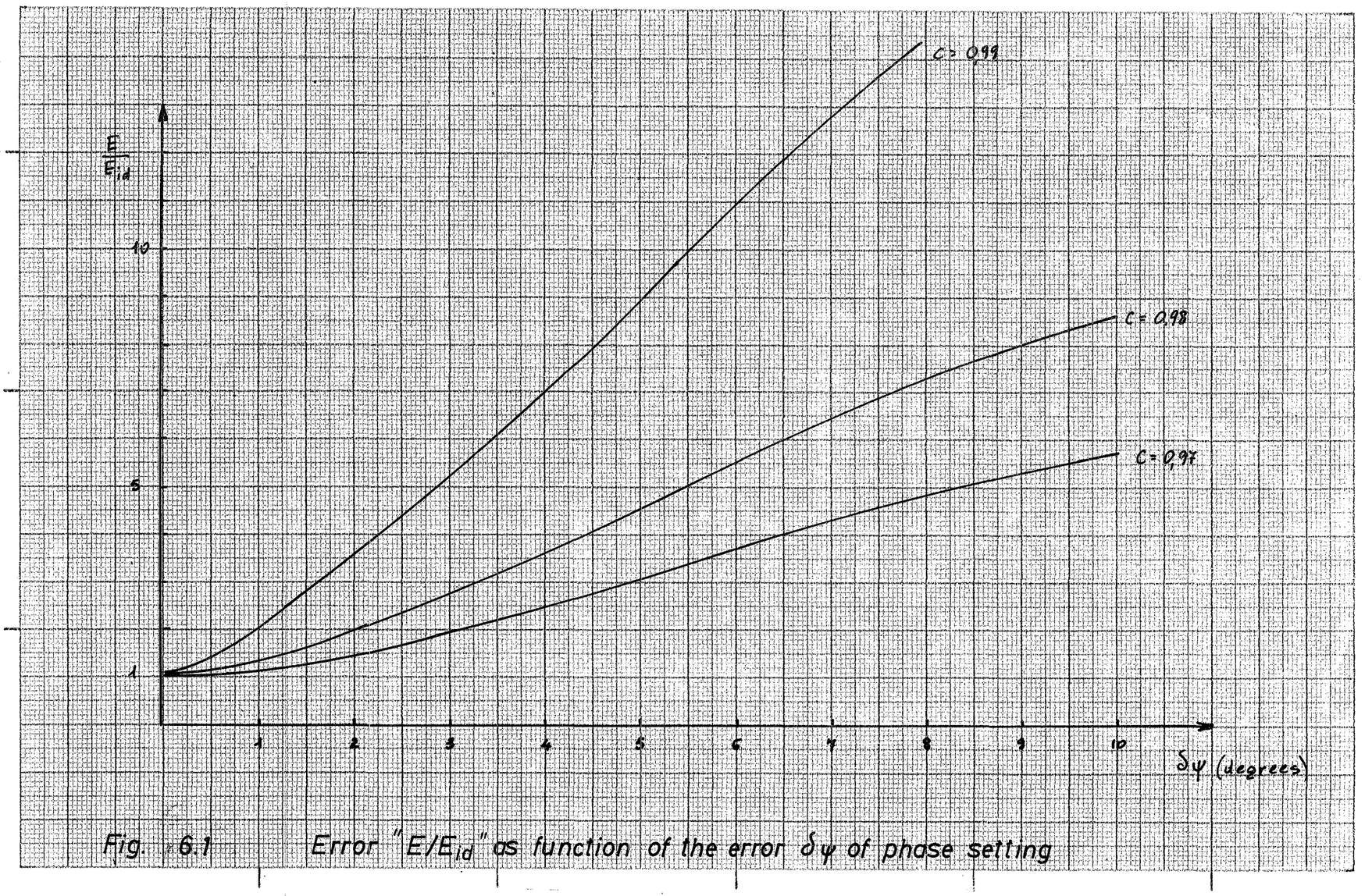

Fig. 6.1 Error "E/E_{id}" as function of the error $\delta\psi$ of phase setting